

ENVIRONMENTAL CONDITIONS AND METEOROLOGIC CONTEXT FOR MODIFICATION OF THE GREAT KOBUK SAND DUNES, NORTHWESTERN ALASKA.

C. L. Dinwiddie,¹ T. I. Michaels,² D. M. Hooper,¹ and D. E. Stillman² ¹Geosciences and Engineering Division, Southwest Research Institute®, 6220 Culebra Road, San Antonio, TX 78238, ²Space Science and Engineering Division, Southwest Research Institute, 1050 Walnut Street, Suite 300, Boulder, CO 80302

Introduction: We are studying meteorologic and niveo-æolian controls on cold-climate sand mobility, transport, and geomorphology at the Great Kobuk Sand Dunes (GKSD) in Alaska [1–5] as potentially analogous to those occurring on high-latitude Martian dunes [2–5 and references therein]. Here we summarize longer-term average meteorologic forcings near the GKSD that are relevant to dunefield modification, and document selected local *in situ* meteorologic data collected in March 2010. In so doing, we estimate the threshold wind speed and demonstrate that debris flow and gully formation on the GKSD, which we observed in the field [5], *does not* require mean daily surface temperatures above or even near the melting point of water.

Setting: The 62 km² GKSD lie ~50 km north of the Arctic Circle and ~160 km inland from Kotzebue Sound within an east-west basin between the Baird and Waring Mountains {Fig. 1 in [4]}. The Waring Mountains are a topographic trap against which dunes climb at the southwestern margin of the field. Many of the dunes migrate west-northwest; we estimated that migration rates fall within the narrow range of 0.5 to 1.5 m/yr [1], which is relatively slow for dunes on Earth. Dune forms include transverse, barchanoid, longitudinal, and star, among others, and range in elevation from 30 to 175 m amsl. The GKSD and surrounding land are vulnerable to accelerating permafrost degradation because the continuous permafrost zone boundary that lies nearby [6–8] is migrating northward in response to a warming climate.

Longer-term climate data: A relatively continuous, ~18-yr time series from the Kavet Creek Remote Automated Weather Station (RAWS; located at 72 m amsl and 3.6 to 19 km from the northwestern and southeastern margins of the dune field) provides relatively long-term meteorologic data {Fig. 1; [9]}. The GKSD experience long cold winters and brief warm summers; mean annual air temperature is -4°C [Fig. 1(A)]. Mean daily air temperature falls to 0°C near the end of September, after nighttime ground frost has returned. Mean daily maximum air temperature falls to 0°C ~2 weeks later, after which air temperature remains below freezing for the season. Mean daily air temperature rises to 0°C near the end of April, after daytime ground thawing has begun. RAWS-measured mean annual precipitation [Fig. 1(B)] is 67% of the PRISM model's estimate [10] at this location; the difference is attributed to snow water equivalent. Snow

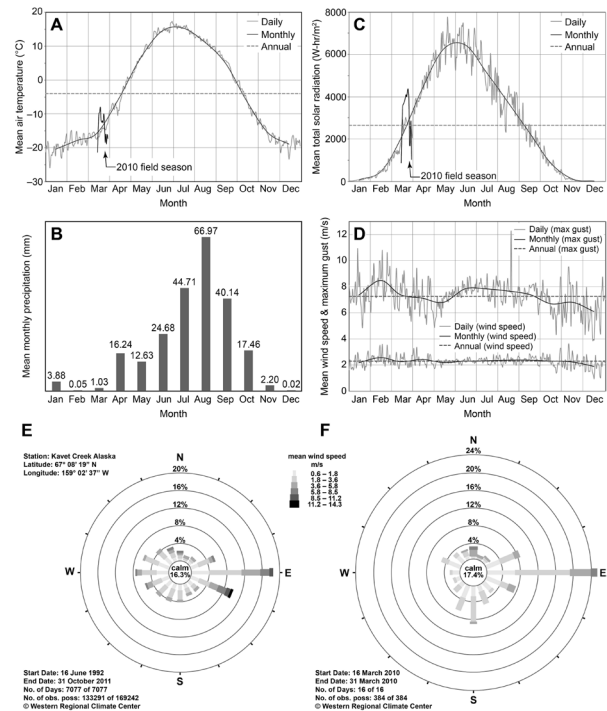


Fig. 1. Kavet Creek RAWS climate data. (A) Mean daily, monthly, and annual air temperature. (B) Mean monthly precipitation. (C) Mean total solar radiation. (D) Mean daily, monthly, and annual wind speed. (E) Mean annual wind rose. (F) Mean wind rose during March 2010 fieldwork. Data credit [9].

partially to fully blankets the dunes for ~70% of the year; rainfall peaks in August.

The strongest daily mean winds are out of the east-southeast from November to April, and average-to-intermediate-strength winds are frequently out of the west from May to July. A mixed wind regime occurs during the transitional months of August–October. Wind speed variance appears to be correlated with solar radiation [Fig. 1(C, D)]; winds are often light and variable during the sunless days of winter, and wind speed variance is lowest during the 38 days of constant summer daylight. The wind regime (measured at 6.1 m AGL) is bimodal at the macroscale [Fig. 1(E)], where the dominant, sand-transporting winds are polar easterlies from November to April (despite snowcover), and a brief westerly wind reversal coincides with summer transport-dampening rains. Active dune migration likely is limited, therefore, to the windy months of early autumn and late winter to early spring. Mean annual maximum wind gust speed is 7.3 ± 1.1 m/s, with gusts up to 40 m/s in the record.

All months except solstitial June and December experience strong but relatively infrequent northerly winds. Significant day-to-day variations in wind direction and strength are commonplace at all seasons due to the quasi-cyclic modulations induced by baroclinic storm systems.

In situ environmental data: We deployed a portable, multilevel meteorological station to three locations {Wx1, Wx2, and Wx3 [4, their Fig. 2 inset]} during our field campaign. This customized system provides the types of boundary layer atmospheric flux data that are needed to assess aeolian erosion potential. We measured 2D (horizontal) mean wind velocity, air temperature, barometric pressure, and relative humidity at 10 sec intervals at 50, 100, and 200 cm AGL, as well as mean net solar radiative flux at 2 min intervals. We also measured ground temperatures at 0, 5, 10, 20, 50 and 100 cm BGL at 2 min intervals, and the number of particle impacts on and kinetic energy imparted to an erosion sensor per 10 sec interval.

Resulting data streams (e.g., Figs. 2, 3) are useful for characterizing microclimates, identifying subgrid-scale processes that influence aeolian transport, and supporting atmospheric modeling (to be demonstrated at the workshop) by providing a measure of whether the nested numerical models capture important processes. Additionally, particle flux data demonstrate sand saltation above snow-free crests (Wx2 and Wx3 locations) and suggest a saltation threshold (Fig. 2).

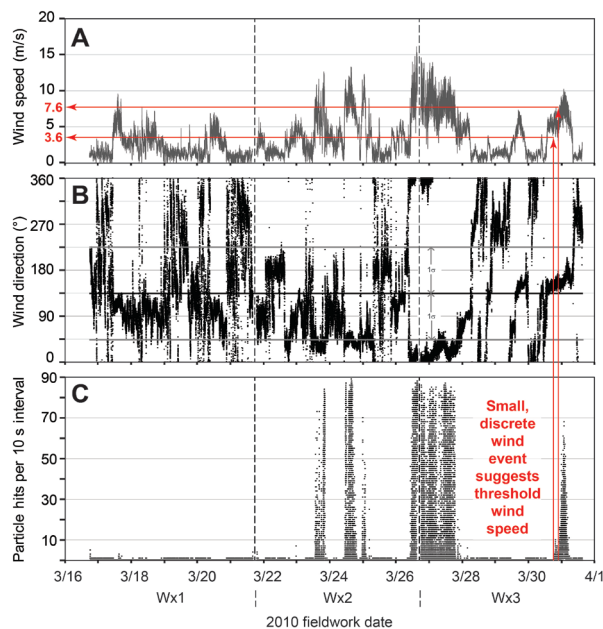


Fig. 2. In situ wind and particle flux data from snow-covered station Wx1 and snowfree stations Wx2 and Wx3. (A) 10-sec mean wind speed at 2m. (B) 10-sec mean wind direction; overall mean azimuth and standard deviation. (C) Particle hits per 10-sec interval. A small, 2.44 hr-long wind event on 30 March had a mean and standard deviation of 5.7 ± 0.7 m/s and caused 504 impacts.

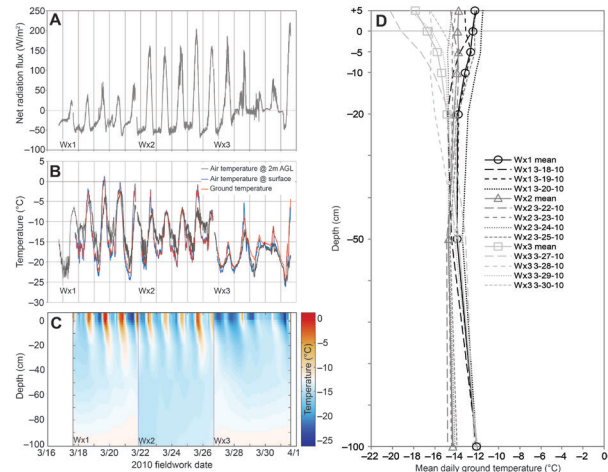


Fig. 3. In situ environmental data. (A) Net radiative flux. (B) Air and ground surface temperatures. (C) Air, surface, and subsurface ground temperatures to 1 m depth. (D) Mean daily air, surface, and subsurface ground temperatures to 1 m depth.

Debris flow observations: Fresh debris flows and gullies on lee slopes were photographed on 25 and 30 March [5] when the mean daily surface temperature was never greater than -12.3°C ; [Fig. 3(C, D)]. Surface temperatures such as these are either colder than or else comparable to austral Antarctic summer temperatures when aeolian Mars-analog field expeditions to that continent are most common.

Conclusions: Meteorologic datasets help elucidate the processes that maintain and sculpt dunefields. The high-latitude, cold-climate GKSD are an excellent U.S.-based Mars analog for cold-season study of dune gully and debris flow processes [5], as well as for study of hydrocryologic controls on high-latitude aeolian transport [e.g., 3, 4]. It is important for in-depth investigations of the GKSD to continue in the near-term, while the arctic analogy is still defensible.

References: [1] Necsoiu, M. et al. (2009) *Remote Sens Environ*, 113, 2441–2447. [2] Dinwiddie, C. L. et al. (2010) *2nd International Planetary Dunes Workshop*, Abstract 2029. [3] Dinwiddie, C. L. et al. (2011) *5th Mars Polar Science Conference*, Abstract 6035. [4] Dinwiddie, C. L. et al. (2011) *XXXXII LPS*, Abstract 2501. [5] Hooper, D. M. et al. (2012) *XXXXIII LPS*, Abstract 2040. [6] Ferrians, O. J. (1965) *Permafrost map of Alaska*. USGS Misc. Geologic Investigations Map I-445. [7] Jorgenson, T. et al. (2008) *9th International Conference on Permafrost*, 121–122. [8] Gruber, S. (2012) *The Cryosphere*, 6, 221–233. [9] WRCC (2011) *Kavet Creek Alaska (RAWS)*. Western Regional Climate Center, Reno, Nevada. [10] Gibson, W. (2009) *Mean Precipitation for Alaska 1971–2000*. National Park Service, Alaska Regional Office GIS Team. Geospatial Dataset 2170508.

Acknowledgements: This research was funded by SwRI[®] IR&D grant 20.R8136 and NASA MFR grant NNX08AN65G, and was subject to U.S. NPS research permit KOVA-2010-SCI-0001. We are grateful to have been provided: data support by S. Stothoff; field support by S. Kantner, R. McGinnis and K. Bjella; logistical support by J. Kincaid; and a private allotment belonging to C. Wood.